A 2DOF THERMOSOLAR CONCENTRATOR PROPOSAL: SOLAR TRACKING AND DISTURBANCE REJECTION USING PROPORTIONAL DEFOCUS.

Diogo O. Machado[1,2], Julio Normey-Rico[1] and Gustavo A. de Andrade[1]

[1] Universidade Federal de Santa Catarina - UFSC, Florianópolis (Brazil)

[2] Instituto Federal de Educação, Ciência e Tecnologia do RS - IFRS, Rio Grande (Brazil)

Abstract

In this work, a novel two-degree-of-freedom linear Fresnel solar collector is proposed. The equipment can vary the power density in the receiver using a proportional geometric defocus besides the conventional solar tracking. This concept was designed to benefit the dynamics and control operations of solar power plants using variable distributed concentration ratio in the concentrating solar collector. For conceptual validation, a numeric scenario of a solar distillation plant with a modified Forristal concentrator operating in a closed-loop fashion with a Filtered Dynamic Matrix Control strategy is presented. Henceforth, is shown the impact of adding this new manipulated variable on the dynamics and control operations. The idea results in a faster actuator which provides both, better performance and operation under constraints.

Keywords: Defocus, 2 DOF solar concentrator, control, MPC, modified Forristal.

1. Introduction

Concentrating Solar Power (CSP) systems are used to transform sun energy to a wide number of applications, such as hydrogen production, heating water systems, electricity generation, liquid waste recycling and desalination. In these applications, the concentrators are used to direct and increase the solar irradiation in the receptor spot and convert it to thermal and electrical energy with the use of a power cycle. The main commercial solar concentrators configurations are shown in Figure 1, where each one of these structures have specifications (Shantia, 2013), advantages and disadvantages (EDF, 2012; Orioli and Orioli, 2011; Kumar, 2015).

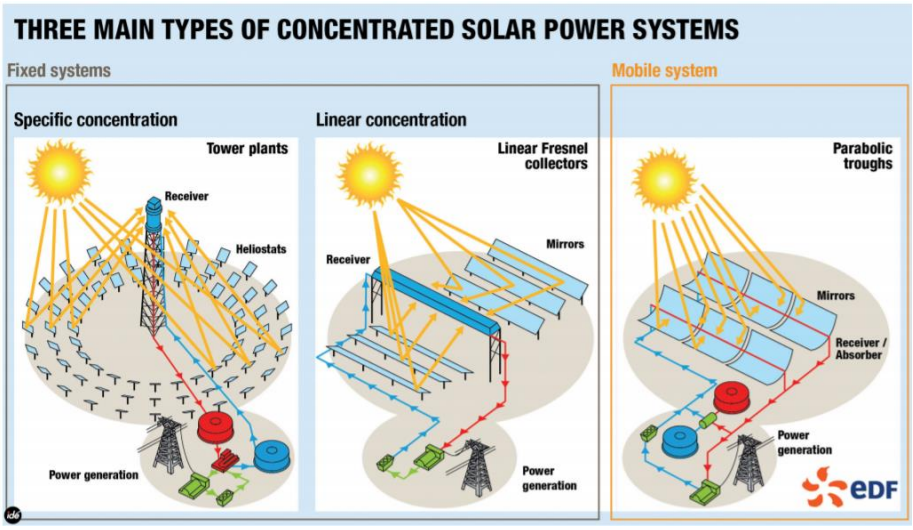

Figure 1 – Common solar concentrators for power generation. Central Tower (left), Linear Fresnel (middle) and parabolic through (right) (EDF, 2012).

Although there are several applications of CSPs, at the present, most systems focus on electricity generation. Solar thermal power plants use the solar energy to heat a thermal fluid by a system of collectors to produce steam in order to feed steam-turbines coupled with generators (Duffie and Beckman 1991). Several disturbances could overheat the system resulting in fluid degradation, premature component failures and performance reduction. Electric power limitations can also be received from the transmission system operator. In this case, the power is decreased by reducing the flow rate leading to an increase in the temperature (Sanches et al 2018). Live steam

Selection and/or peer review under responsibility of Scientific Committee
doi:10.18086/swc.2019.01.05 Available at http://proceedings.ises.org

parameters have a strong influence on the life span of the steam turbines, an expensive asset, and unlike in plants supplied by fossil sources, the steam supplied from solar thermal power plants varies depending on the irradiation (Willwerth et al., 2018). In this sense, mechanisms to deal with these conflicting issues are the interest topic of this research.

Regardless of the CSP application and technology, there are situations where it is necessary to defocus the solar concentrator for safety, operation, optimization or maintenance of the system. The most classic examples of such scenarios are in the occurrence of storms, strong wind and high solar radiations. Thus, the concentrator defocus is an important operational alternative for safe and cost-effective plant operations. Nowadays the industrial concentration systems only have total or partial defocus options, and the latter is made using the solar tracking in parabolic troughs mechanism to change the optimum relative angular sun incidence.

From the industrial process control perspective, the work fluid flow (control variable) inside the absorber tubes of the solar concentrator is manipulated, by means of a radial pump, in order to maintain the outlet temperature (controlled variable) around the desired set point. The most common disturbances for the control system are the solar irradiation, pressure fluctuations, ambient temperature, optical efficiency and inlet temperature of the working fluid. Another interesting aspect is the transport lag, once the temperature sensor is located at the collector outlet and the pump is installed at the inlet. This implies that the temperature will be affected by the flow of previous time instants, due to the residence time of the fluid inside the collector.

In this topic of research, Araujo (2018) proposed a modification in the solar concentrator control system. Basically, a new binary variable was included in the computation of the control law by means of a non-linear model predictive control formulation. This variable was used to deal with total or partial mirror defocus considering the actual solar tracking mechanism technology, thereby, the partial defocus operates advancing or lagging the relative angular focal point to the irradiance angle. Although, the focal angular change can generate thermal and mechanical stress due to irregular temperature gradient in the absorber (Steinman and Eck, 2000). However, these authors did not consider a detailed study of the collector optical aspects (Zheng et al., 2014). The system used for conceptual evaluation is the thermal absorption model presented in the works of Torrico et al. (2010) and Lima et. al (2016). These articles applied control techniques in a solar system of a desalting plant.

This work proposes the addition of one more degree-of-freedom (DOF) in solar concentrators control systems permitting the focal manipulation and consequently, the energy absorbed in the receiver tube. This can be performed varying the aperture area/absorber ratio or the energy density in the absorber area related to the direct normal irradiation (DNI). The system is a two-degree-of-freedom control actuator linear Fresnel solar collector which is capable of proportional defocus and solar tracking simultaneously. Because of the mechanical nature of Fresnel modules and the distributed construction of a solar field, is expected that adding this manipulated variable to the control system could enhance performance maintaining safety. Although, in this approach only the defocus is evaluated. The Filtered Dynamic Matrix Controller (FDMC) multi-input multi-output (MIMO) was chosen to validation because it is a modification of DMC, widely used in industry (Normey-Rico and Camacho 2007) dealing with variable dead-time, multiple variables and considering constraints at project phase. So, a mathematical model of this new Fresnel module is made in section 2, while in section 3 the solar field model is defined, in section 4 the control specification and logic are stated. In the section 5, the response results are described with this novel concentrator to validate the concept, and, finally the conclusions are stated in section 6.

2. Fresnel 2DOF

This section is based on the work of Ozturk (2011) and presents the basic geometric concepts of parabolic through and linear Fresnel concentrators.

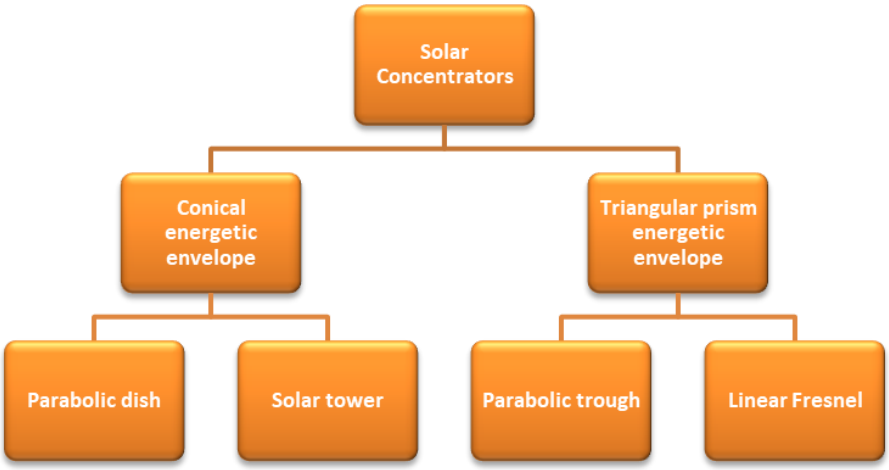

Figure 2- Solar collector classification to the energetic volume. Modified from Ozturk (2011)

Figure 2 shows a classification of solar collectors based on the created energy volume because of the geometric nature of collectors. This definition was modified once, in one hand, the disc collectors directs the incident irradiation to a focal point and, in the other hand, the parabolic through forms a focal line. Therefore, it happens that the commercial collectors are designed to coincide the absorber in the same point of the optical focal point, thereby, all the incident irradiation in the mirror area is directed to the collector. Although, if the mirror could in some way change its format it would be possible to change its focal point, or line, and, therefore, change the power density in receptor or vary the aperture/receptor areas ratio. This idea is presented in the graphics of Figure 3.

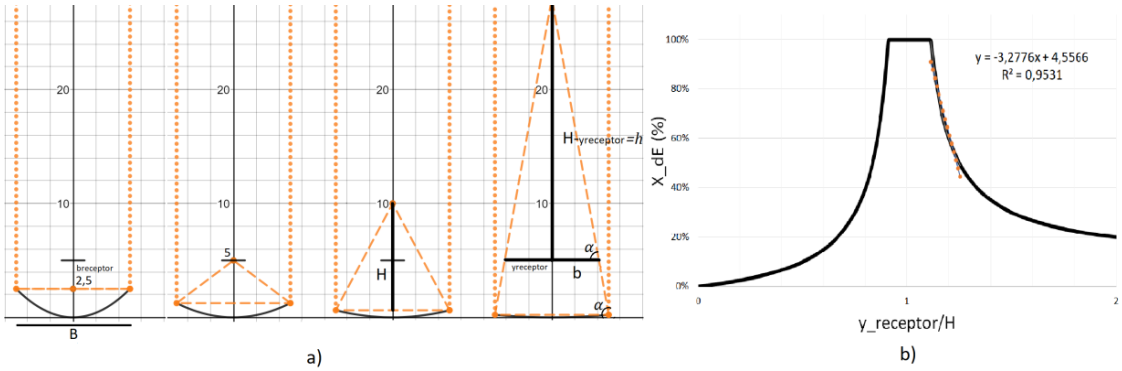

Figure 3 – Transversal cut in a parabolic through collector with constant area and different focal points. (a) First case is a focal point below the receptor height. Second case is a coincident receptor height and focal point (100% concentration). Third and fourth case are different concentration ratio, or energy density in the triangle prism cut in the receptor height due to focal point position variation. (b) is the sensitivity analysis of the variation depicted in (a) with respect of the normalized power density. Full concentration case is in the $y_{receptor}/H = 1$. The left side represents the focal point variation below the receptor height while the right side represents the focal point above the receptor height. The saturated wide section depends on the receiver wide.

Thereby, if the receptor is not in the same distance of the focal point a ratio between collector aperture area and receptor area governs the energy transfer to the work fluid, or, an area of a pyramid energy trunk coincides with the receptor height. The incident energy on the receptor, if the focal point is coincident with the receptor height, is given by Forristal (2003) *apud* Shantia (2013) equation:

$$\dot{q_{Sol}}_{abs} = \dot{q}_{\iota}\eta_{abs}\alpha_{abs} \qquad \text{(eq.1)}$$

where $\dot{q_{Solar}}_{abs}[W/m^2]$ is the solar heat incident in the receptor, $\dot{q}_{\iota}[W/m^2]$ is the solar irradiation, η_{abs} is the optical efficiency and α_{abs} is the mirror absorption factor.

For the case in which the focal point does not coincide with the receptor, there is an aperture/absorber area ratio, and for simplification and model usage, for now on it will be considered prism energy envelopes relationships, thereby, parabolic through and linear Fresnel collectors are defined. Considering the schematic of Figure 3, and

hypotheticals A mirror width of 10 m and receptor B of 2 m, in first case (a) is possible infer that all incident irradiation is concentrated in the receptor, or absorber, and, therefore, the concentration is of 100%. In the sequence cases of (a) the energy density plane that cut the triangular prism on absorber height is diminished with the increase of the triangle height and is approximated considering the relations of eqs. 2, 3, and 5, of the rectangles triangles that compose the isosceles triangle of the last case on Figure 3a.

$$tg(\alpha) = \frac{2H}{B} = \frac{2h}{b} \quad \text{(eq. 2)}$$

$$h = H - y_{receptor} \quad \text{(eq. 3)}$$

$$b = \frac{B(H - y_{receptor})}{H} \quad \text{(eq. 4)}$$

$$X_{dE} = \frac{b_{receptor}}{b} = \frac{b_{receptor}}{B} \frac{H}{(H - y_{receptor})} \quad \text{(eq. 5)}$$

$$\dot{q}_{Solabs} = \dot{q}_{\iota} X_{dE} \eta_{abs} \alpha_{abs} \quad \text{(eq. 6)}$$

So, for a variable energetic density and constant absorber width the total absorbed energy will vary. Thereby, it would be possible to use the defocus system not just for safety cases but also for disturbance rejection. The collector aperture area and the triangle prism cut area at absorber height could be related to the irradiation fraction which is effectively concentrated by the mirrors to the absorber. Thereby, is possible to change the Forristal eq. 1 to a modified one, eq. 6, that considers the proportional defocus or aperture / absorber areas ratio.

From the Forristal modified equation and the hypothetical configurations is plotted the graph which considers $\dot{q_{Solabs}} = f(H/y_{receptor})$, thereby, the absorbed heat in receptor is a function of the ratio between the focal point height and the absorber height, this sensitivity analysis indicate agreement between the simulated results with a more detailed model of Ozturk (2011). Also, in the position which is installed the receptor occurs a dead band with full absorption, this happens because the absorber width, once the focal plane must be greater than the absorber area to the ratio begins to change. For a negative displacement, considering the absorber in the origin, if the focal point is below the absorber height there is a decrease in the energy density until it reaches zero, this point has an analogous behavior with the positive displacement. In the case which the focal point is above the absorber height the energy density values drop to the absorber area/aperture area ratio which is 2/10 meters or 20%.

Although, the practical problem to vary the focal point of rigid mirrors that composes commercial solar concentrators could restrict it construction. Is technically challenging to dynamically vary the shape of a whole solar concentrator mirror because of the mirror material nature and the actuation system. Considering these restrictions is proposed the utilization of Fresnel collectors. Fresnel collectors are composed by various mirror stripes disposed in a flat linear composition, in which each mirror could be independently positioned. In solar tracking systems the mirrors could one by one adapt its angles depending on the solar irradiation angle to enhance the concentration on the absorber for a given solar angle. Therefore, the defocus usually is to flatten only the mirrors, in other hand, parabolic throughs uses on-off mode or leading and lagging the whole structure for solar tracking position. The last option could generate non-uniform heat distribution and mechanical stress (Steinman and Eck, 2000). Also, commercial flat Fresnel mirrors are mechanically coupled to reduce costs and increase design simplicity. In these conditions, just one motor is needed for the coupled mirror mechanism to be able to adjust the mirrors angles due to solar tracking. Once the Fresnel concentrator utilizes plane mirrors and each one could operate independently is possible to extrapolate its common or commercial operation to vary its focal point in the logic of the presented logic. Considering the differences of the two concepts, the first step is to correlate the Fresnel operation to the parabolic troughs in a way that connects the variable focal point collector concept and the Fresnel collector construction flexibility.

In Figure 5a is demonstrated the discretization of a parabolic concentrator. This is done in small parabolic mirror intervals on the parabolic surface. In 5b the trimmed mirrors are grouped over a plane surface in $y = 0$. Although, the angles direct the irradiation in different focal points once the global surface of mirror are not positioned along a parable anymore, but in a horizontal line at the origin. Therefore, is necessary an adjustment in the relative mirrors angles for the system to have a coincident focal point. So, if is possible to correlate the angles between the mirrors on the Fresnel module to have a common focal point, therefore, is possible to add one more mechanical actuator and propose a 2 degrees of freedom (DOF) Fresnel collector which operates varying the focal point,

thereby, governed by the modified Forristal eq. 6.

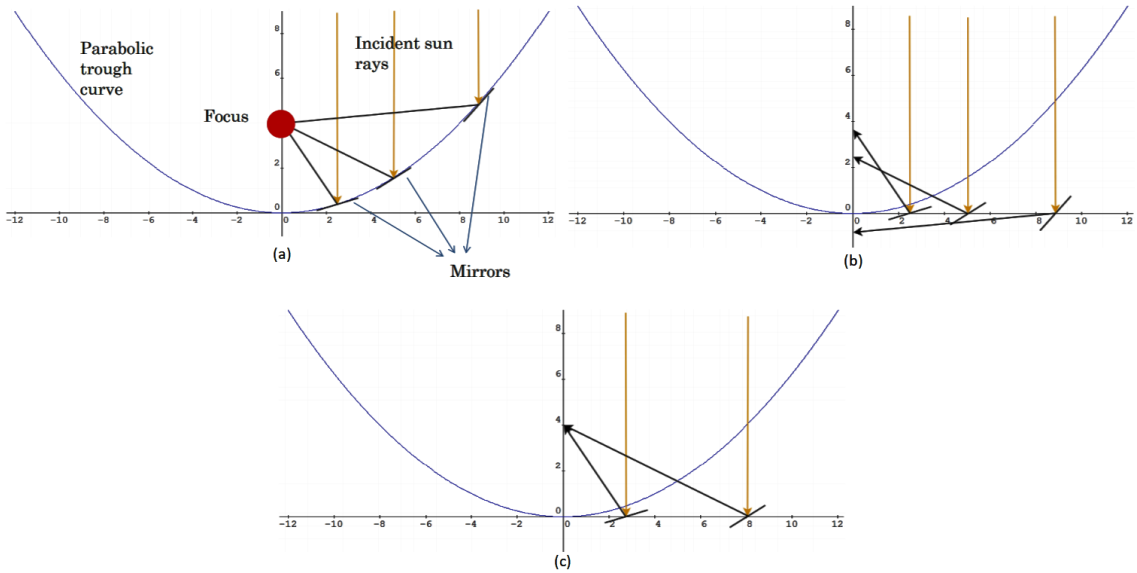

Figure 4 – Geometric transformation of parabolic through to linear Fresnel (Ozturk,2011). (a) cut the parabolic mirror in small plane sections. (b) Translation of the plane mirrors a plane in origin. (c) relative angle correction to coincide the focal point of the discretized mirror.

In this sense, is stated the logic of the a 2DOF Fresnel solar collector concept and viability. The equipment that is not just dynamic capable to actuate during transients for control purposes but also to operate in safety and process limits. To reach this synergic objective is necessary a control technique which considers the constraints in design phase and the dead time nature of the solar thermo fluid dynamic process. For this motive, in this conceptual proof is used a filtered predictive controller. The shading and block effects on the collectors that impacts the plant operation are not considered (Zheng et al., 2014).

3. Solar field definition

The system used for conceptual analysis of the 2DOF Fresnel collector proposed in this work is the desalting plant AQUASOL (Roca et. al, 2008a, 2008b). This plant is located at the Plataforma Solar de Almería, Spain, and it is used to desalt water with solar thermal energy. It is composed by a compound parabolic concentrator solar field, storage tanks, multi-effect distiller with 14 stages and an absorption heat pump. The plant optimal operation point is at 66.5 ºC in the first cell, and it can operate in 3 modes: solar, fossil or hybrid heating. The solar field work fluid is water, and the field is made up of 252 collectors with an area of roughly 500 m² in 4 loops of 63 collectors. There are collectors connected in parallel in seven groups three by three, as can be seen in Figure 5.

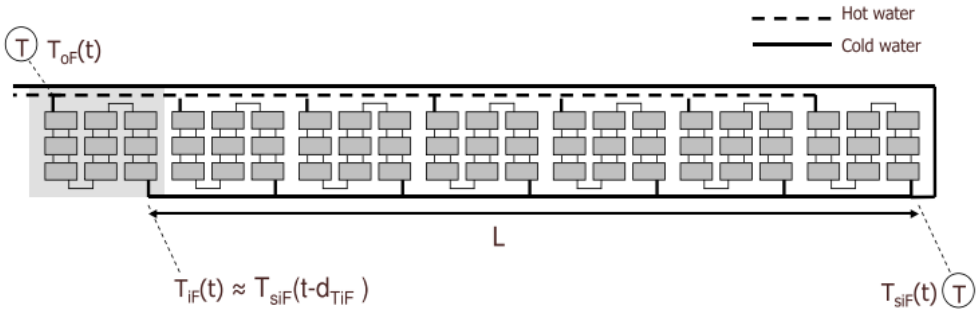

Figure 5 – AQUASOL desalting plant solar field structure. One loop is composed by 7 groups with 3 parallel connections and 7 collectors each (Torrico et al.,2010).

The system detailed description, modelling and validation is available in Roca et. al (2008a, 2008b). The dynamic model of the water temperature at the output of the solar collector field is given by the following equation:

$$\rho C_p A_a \frac{\partial T_{OF}(t)}{\partial t} = \beta_I I(t) - \frac{H}{Leq}(\bar{T}(t) - T_a) - C_p \dot{m_{eq}}(t - d_c)\frac{T_{OF}(t) - T_{iF}(t)}{Leq} \quad \text{(eq. 7)}$$

For the computation of $\dot{m_{eq}}$ it has to be taken into account the number of operational loops in the solar field (n_l), number of colectors in each loop (n_c), number of parallel conections (n_{cp}) and the number of absorbers in each collector (n_a):

$$\dot{m}_{eq} = \frac{\dot{m_F}}{n_l n_c n_{cp} n_a}$$

Table 1 - Models parameters and operations points (OP).

Symbol – Name	Value	Symbol - Name	Value [limits]
ρ- Water especific mass	975 (kgm^{-3})	n_{eq}- Collectors parameters	5.88
C_p- Specific thermal capacity	4190 ($Jkg^{-1}ºC^{-1}$)	L_{eq}- Absorber tube length	5.67 (m)
A_a- Cross-section area	1.745e-4 (m^2)	$\bar{T}_{OF}$- Out temperature OP	
β_I- Irradiance parameter	0.1024 (m)	$\bar{T} = \frac{T_{OF}(t) - T_{iF}(t)}{2}$	20.42 [5-25] (ºC)
H- Termal losses coefficient	4 ($Jkg^{-1}K^{-1}$)	$\bar{\dot{m}}_F$- Mass flow OP	2.55 [1.2,4.4] (L/s)
L_{eq}- Absorber tube length	5.67 (m)	$\bar{I}$- Irradiance OP	800 (W/m^2)
d_c- Mass flow I/O dead time	40 [30,50] (s)	$\bar{X}$- Focus energy OP	100 [50,100] (%)

In this context is proposed a modification on the eq. (7) which represents the mathematical description of the 2DOF Fresnel collector idea. This modification adds the proportional variation of the energetic density in a hypothetical Fresnel collector as depicted by the eq. (6) and Figure 3a. Is important to say that the AQUASOL utilizes parabolic trough. In this sense, the collector parameters are well known and were used in this conceptual analysis, even knowing that the collector proposal is possible considering a Fresnel structure. So, the resulting model equation presents a new $X(t)$ variable related to the new working logic, so eq. (7) was modified in this work to count on the proportional defocus:

$$\rho C_p A_a \frac{\partial T_{OF}(t)}{\partial t} = \beta_I I(t) X(t) - \frac{H}{L_{eq}}(\bar{T}(t) - T_a) - C_p \dot{m}_F(t - dc)\frac{T_{OF}(t) - T_{iF}(t)}{n_{eq} L_{eq}} \quad \text{(eq. 8)}$$

were the percentual defocus, $X(\%)$, was added with mass flow $\dot{m}_F(L/s)$ as manipulated variables. The controlled variable is the outlet temperature of solar field $T_{OF}(°C)$, and disturbances are irradiation, $I(W/m^2)$, ambient temperature $T_a(°C)$, and inlet temperature of the field T_{iF} $(°C)$, other parameters are available in Table 1. The energy density is operated in the range of 50-100% because of the nonlinear behavior showed in Figure1 b.

The next steps to execute the simulation of the eq. (8) and to run the controller tests are the linearization and discretization. The linearization method is the forward approximation of the derivative and the operational points, therefore, linearization point, are defined in Table 1. The linearized equation resulted in:

$$\Delta T_{OF}(t) = \Delta T_{OF}(t-1) + a[\Delta I(t-1) + \bar{I}\Delta X(t-1)] - b[\Delta T_{OF}(t-1) + \Delta T_{iF}(t-1) - 2\Delta T_a(t-1)] + c[-\bar{m}_F \Delta T_{OF}(t-1) + \bar{m}_F \Delta T_{iF}(t-1) + (\bar{T}_{iF} - \bar{T}_{OF})\Delta m_F(t-1-d_c) \quad \text{(eq. 9)}$$

With this, applying the z transform, the final numeric discrete transfer function is described in eq. (10):

$$\Delta T_{OF}(z) = \frac{-0.18\, z^{-8}}{z-0.98}\Delta \dot{m}_F(z) + \frac{0.57}{z-0.98}\Delta X(z) + \frac{0.72e-3}{z-0.98}\Delta I(z) + \frac{0.02}{z-0.98}\Delta T_{iF}(z) + \frac{0.49e-2}{z-0.98}\Delta T_a(z) \quad \text{(eq. 10)}$$

All in all, the system is a multiple-input single-output MISO process. Where T_{OF} is the controlled variable, $\dot{m}_F$ and X are the manipulated variables and I, T_{iF}, T_a are the disturbances. Considering this structure, a Filtered Dynamic Matrix controller is discussed next.

4. Control Definitions

In this work, the authors propose the use of the FDMC strategy with two manipulated variables: the standard one, the inlet fluid flow, and a novel one, the proportional defocus, possible through the 2DOF Fresnel collector

described in Section 2. The work of Lima et al. (2015) describe details of the application of the FDMC in the context of solar plants. The dynamic behavior of the AQUASOL plant presents some challenges for the control design due to the location of the temperature sensor and the pump, leading to delays for different input or output variables. In Normey-Rico and Camacho (2007), the authors showed that the Dynamic Matrix Controller (DMC), a model predictive control strategy, implicitly uses a Smith predictor (SP) structure, a famous dead time compensator (DTC) structure. Also, these authors propose the inclusion of a first order filter in the SP structure, in order to improve the poor disturbance rejection capabilities and lack of robustness properties of the original SP.

This technique has become well-known in literature as the filtered Smith predictor (FSP). In this context, Lima et al. (2014) suggested a modification of the standard DMC to merge the Filtered Smith Predictor and the Dynamic Matric Controller advantages. With this, the resulting FDMC tuning procedure have one more degree of freedom to adjust disturbance rejection and robustness. More proofs and example about robustness and rejection are available in the base article (Lima et al. 2016) as well as the recursive implementation used in this work. Some additional advantages of FDMC are the parameter tuning simplicity and practical implementation, since the algorithm needs minor changes of the industry standard DMC.

Basically, the FDMC technique seeks to minimize the following cost function J:

$$J = \left(\hat{\Upsilon} - W\right)^T Q_y \left(\hat{Y} - W\right) + \Delta u^T Q_u \Delta u \qquad \text{(eq. 11)}$$

where Q_y and Q_u are diagonal matrices that represents the weights of future errors and future control increments. And W is the future reference vector while $\hat{Y}$ is the predictions process variable vector in a chosen horizon. For the calculation of $\hat{Y}$ is defined eq. 12:

$$\hat{Y} = G\Delta u + H\Delta u(t-1) + H_n \Delta n(t) + 1\hat{y}(t + d_n|t) \qquad \text{(eq. 12)}$$

where G, H and H_n are matrices $N_y \times N_u$, $N_y \times M$ and $N_y \times M + 1$, N_y and N_u are the prediction and control horizons and M is the number of step coefficients of the input-output and disturbances-output responses. So, $\hat{\Upsilon} = \left[\hat{y}(t + d_n + 1|k), \dots, \hat{y}\left(t + d_n + N_y\middle|k\right)\right]^T$, the future increment vector $\Delta u = [\Delta u(t), \dots, \Delta u(t + N_u - 1)]^T$, the past control increments $\Delta u(t-1) = [\Delta u(t-1), \dots, \Delta u(t + N_u - 1]^T$, and finally the measurable disturbance $\Delta n = [\Delta n(t), \dots, \Delta n(t - M)]^T$. For a compact description of the predictions, the eq. 12 can be separated in free and forced response:

$$\hat{Y} = G\Delta u + f \qquad \text{(eq. 13)}$$

where f contains all the terms which are not affected by the control actions, therefore, the free response is the process response if no control action is made. The term $G\Delta u$ is the forced response and represents the process response due to future control actions. The Δu is calculated through eq. 11 and in a case which all future references are constant, $W = 1r(t)$, and with no constraints, an algebraic equation solution emerges for $\Delta u = K(W - f)$. Further mathematical manipulation can be done to show that the control signal $u(t)$ could be obtained by the equation:

$$U(z) = C(z)\left(R(z) - \hat{Y}(z)\right) + C_{ff}(z)N(z) \qquad \text{(eq. 14)}$$

Concluding, this means that the DMC controller can be represented by a classical control scheme. It has a primary feedback controller that considers the reference and prediction error in a control horizon, also, a feed-forward controller like depicted in Figure 6.

All in all, the predictor structure is used to obtain the expected value of the outputs after the dead time. So, some modifications are made to count on the transport lag of the process. Considering $G_{DMC}(z)$ and $G_{pDMC}(z)$ as the nominals models shifted for a dead-time number of samples for a step response of the system.

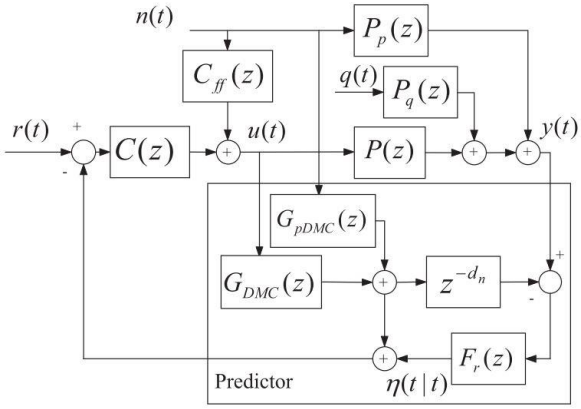

Figure 6 - Block diagram of the DMC interpreted as a DTC structure with feed-forward (Lima et al., 2016). This predictor structure merges the advantages of FSP and DMC.

The structure of Figure 6 is characterized by an FSP structure, where $n(t)$ is the measurable disturbance, $q(t)$ is an unmeasured disturbance that affects the process through $P_q(z)$. Defined the structure some behaviors are highlighted:

- Measurable disturbance rejection in the nominal case, $G_{pDMC}(z) \cong z^{d_n} P_{pn}(z)$, where P_{pn} is the nominal disturbance-output transfer function. The rejection will be only dependent of $C_{ff}(z)$ and $C(z)$, this happens because the filter $F_r(z)$ do not have effect on the response for the perfect prediction.
- Measurable disturbance rejection in the dead-time error case, $G_{pDMC}(z) \neq z^{d_n} P_{pn}(z)$. The prediction on $t + d_n$ will be an approximation.
- No available disturbance measurement case. Considering the filter $F_r(z) = 1$, the original DMC algorithm is equivalent to the SP. Therefore, the issues about disturbance rejection will be sustained, or, if the tuning is made to improve set-point tracking the robustness could be compromised.

5. Results

In this section, two days data are simulated and compared to the published results of Lima et al. (2014) using the FDMC controller with and without the proposed 2DOF Fresnel collector. The tuning guidelines were the same for the two cases. $N_y = 50$,$N_u = 10$ and $Q_u = \lambda_n K_p^2$, where K_p is the gain of the nominal model and $\lambda_n = 1$. Where the Q_u was normalized because the selection of the λ_n does not depend on the process gain (Normey-Rico and Camacho, 2007). The nominal values of the linearization and for the simulation are described in Table 1. Also, a low-pass filter was used for attenuation of noise effects:

$F_r(z) = \frac{0.15}{z-0.85}$

The main purpose of the control system is to maintain the difference of the inlet and outlet temperatures within the range of 5-20ºC to optimal collector efficiency and less material stress due to the temperature gradient. The process delay was set in 40 s, thereby, 8 sample times, with variation of ± 10 s depending on the mass flow. In the simulation time there was changes in the temperature setpoints as can be seen in upper plot of Figure 7 and 8.

So, the two simulation scenarios are depicted in Figure 7 and 8. The upper plot shows the setpoint, the 1DOF and the 2DOF responses outlet temperature profiles, or the controlled variable. The middle plot has two y axis, were the left axis is the manipulated variable field flow, the black continuous and dashed lines are the flow profiles for the 2DOF and 1DOF structure respectively. Right y axis is the second manipulated variable that is the normalized energy density in orange continuous line. So, the middle plot depicts the manipulated variables. Finally, the bottom plot presents the disturbances profiles that are from real data of the AQUASOL plant. It is composed by the ambient temperature, inlet water field temperature and by the Direct Normal Irradiation.

In Figure 7 the irradiation follows the day normal distribution until almost the 2500 sample, were it gets perturbed. The ambient temperature shows a ramp from 250 to 750 and suddenly drop its value. The inlet water field

temperature stays stable along the simulation. Is evidenced the fast actuation of the mechanical system of the proportional defocus varying the energy density in comparison of the pump actuation to change the field inlet flow on the middle plot. Also, the collector actuation varies the irradiation of the whole field while the mass flow has a greater dead time depending on the temperature sensor location and velocity. In top plot the dashed black line is related to the 1DOF collector and it is farthest from the set point orange dashed line in comparison of the black continuous line of the 2DOF concept collector. An interesting behavior is that the inlet field flow for 1DOF collector is lower than the 2DOF this results in a greater gain for the proportional defocus, although, the total energy converted decreases once the outlet mass flow is lower for a given temperature.

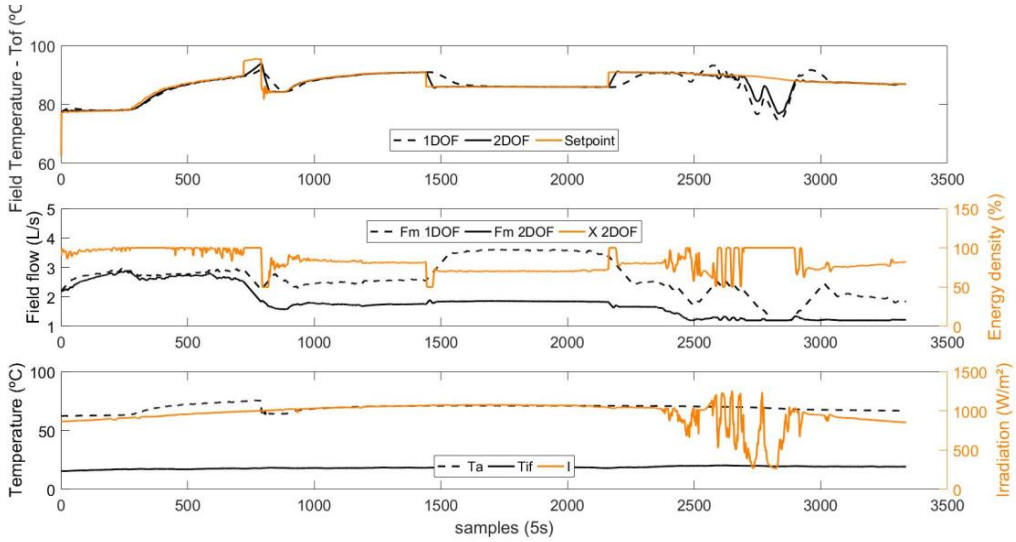

Figure 7 – Data set 1 – Top plot is controlled variable. Middle plot are the manipulated variables. Bottom plot are the disturbances.

In Figure 8 is possible to see a normal irradiation until sample 1500. Between 1500 and 2000 there was an irradiation disturbance and after 2000 the irradiation become very low and noisy. The ambient temperature had a negative step between 500 and 1000 and is steady in the rest of the data set, also the inlet temperature stayed stable in all simulation. The manipulated variables can be evaluated with the middle plot. It is possible to compare the field flow with the 2DOF Fresnel collector and with the 1DOF. Also, the impact of the proportional defocus varying from 50-100%. The operation can be discussed based on the upper plot, which represents the 1 DOF performance with the dashed line and the 2DOF with a continuous line. By inspection of the plot is evident that the 2DOF actuator can maintain the temperature at the setpoint better than in the 1DOF case. Also, for an increase

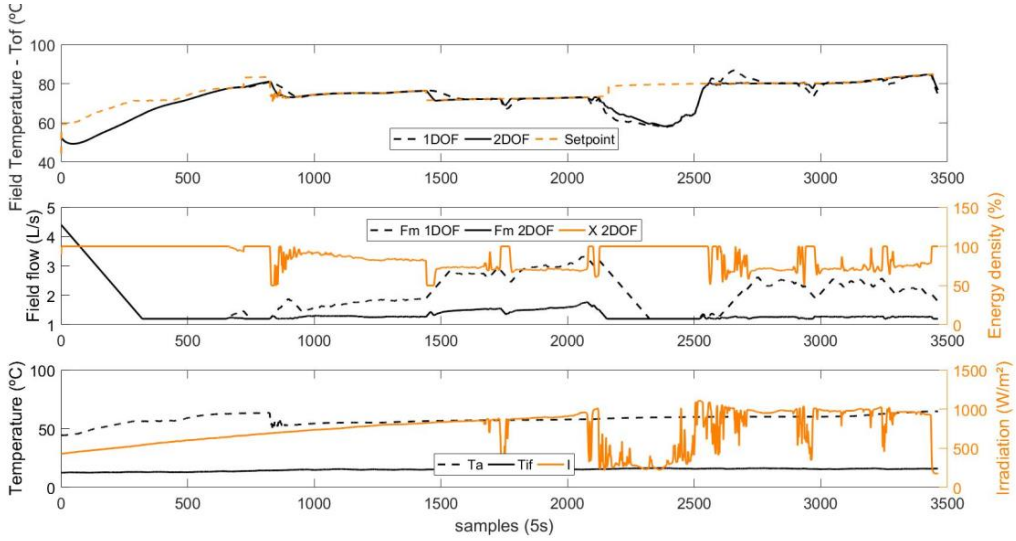

Figure 8 - Data set 2 – Top plot is controlled variable. Middle plot are the manipulated variables. Bottom plot are the disturbances.

in temperature the two concepts have the same behavior, although, in the cases of decreasing irradiation the 2DOF have a better response to track the setpoint because the field flow is lower, leading to a greater gain for the focus/defocus operation considering less mass in the absorber. In 2500 to 3500 is possible to evaluate that the defocus mechanism can deal with the fast irradiation disturbances, also, in the 1DOF case, the field mass flow has slower dynamics resulting in more variation in the Field Temperature. Other interesting behavior is from 2000 to 2500 samples, were the energy density stayed saturated at 100% because of the low irradiation, even with the temperature decrease. To sum up, Table 2 depict the IAE index:

Table 2 - Integral of Absolut Error (IAE) index for the two data sets depicted in Figure 7 and 8.

	1DOF Fresnel	**2DOF Fresnel**
Data set 1	7.9545e+03	5.3968e+03
Data set 2	16.105e+03	13.460e+03

6. Conclusions

This work is an effort to connect different advantages of different areas to reach a simple, yet powerful, idea of 2DOF collector. Firstly, is stated the basic functioning of parabolic trough collectors and the geometric nature of a parable mirror. After, is defined a hypothesis of a variable focal point collector and, them, is used the Fresnel linear collector construction characteristics to connects the idea of a variable parable to a feasibility collector that is described by a modified Forristal equation. After, the AQUASOL desalting plant is presented and its models are modified to embed the idea of a collector for disturbance rejection. Then, is stated the control algorithm and the basic idea behind FDMC. Two real data sets are used to run the simulation. The two compared control structures can reject the disturbances, and results section generated some relevant advantages:

- The IAE index of the 2DOF collector is less than the same index o 1DOF, which implies in a faster setpoint tracking of the proposed collector.
- The proposed 2DOF collector have smaller constant times than the inlet field flow, therefore, the collector has better dynamic responses operating in higher frequencies. So, the control system has capacity of reject a wider range of disturbances.
- Due to the tuning and weighting of the DMC is possible to change the response behavior of the 2DOF case. Although, to the comparison purpose the tuning were equivalent.

The main disadvantage of the 2DOF collector operation with the inlet field flow is that the flow could operate in lower levels respecting the desired temperature set-point. In this sense, the total energy output of the solar field is lower once the calculation of the total energy is made multiplying the mass, temperature and specific heat of the work fluid. So, in many cases of Figure 7 and 8 in which the both actuators are not saturated at maximum, is possible to optimize the outlet energy.

For future works this relation should be evaluated and a solution to maximize the energy output with the temperature constraints should be developed.

7. Acknowledgments

This work has been developed within the context of all activities related to the R&D project registered with ANEEL under the code PD-00553-0042/2016 and sponsored by Petroleo Brasileiro (PETROBRAS).

The authors are thankful for the financial support from Petrobras/ANEEL and for the capacitation support of Instituto Federal de Educação, Ciência e Tecnologia – IFRS – Campus Rio Grande.

J. E. Normey-Rico thanks CNPq for financial support, project 305785/2015-0

8. References

Willwerth, L., Feldhoff, J.F., Krüger, D., Keller, L., Eickhoff, M., Krüger, J., Pandian, Y., Tiedemann, J., Succo, M., Khenissi, A., 2018. Experience of operating a solar parabolic trough direct steam generation power plant with superheating. Sol. Energy 171, 310–319. https://doi.org/10.1016/j.solener.2018.06.089

Araujo, T. D. Costa, P. R. C. Noremy-Rico, J. E. and Bordons, C. Optimal Solar Collectors Defocusing Based on Maximum Temperature. 9th International Renewable Energy Congress (IREC). DOI: 10.1109/IREC.2018.8362488. Isbn: 9781538609989. Hammamet, Tunisia. March, 2018.

EDF. Technolgy unveiled - concentrated solar power. n. June, 2012.

Kumar, R. Solar Thermal Technologies for Power Generation in India. v. 2, n. 6, p. 41–44, 2015.

Forristall, R. Heat Transfer Analysis and Modeling of a Parabolic Trough Solar Receiver Implemented in Engineering Equation Solver. n. October, 2003

Orioli, F. S.; Orioli, V. S. Parabolic or Fresnel ? 2011. Disponível em: <www.soltigua.com/wp-content/uploads/2009/09/Soltigua{\\ _}Energetica{_}ind>.

Özturk, A. Sensitivity of Energy Yield of CSP Systems with Fresnel Mirrors to Structural Parameters. 2011.

Shantia, A. Low cost / high performance Linear Fresnel Receiver design for Concentrated Solar Power applications. Master thesis, KTH. Stockolm. 2013.

Torrico, B. C. et al. Robust nonlinear predictive control applied to a solar collector field in a solar desalination plant. IEEE Transactions on Control Systems Technology, v. 18, n. 6, p. 1430–1439, 2010. ISSN 10636536.

Lima DM, Normey-Rico JE, Plucênio A, Maia TL. Improving robustness and disturbance rejection performance with industrial mpc. In: XX Congresso Brasileiro de Automática (CBA); 2014. p. 3229–3236. ⟨http://www.swge.inf.br/CBA2014/anais/PDF/1569926319.pdf⟩

Lima DM, Normey-Rico JE, Maia Santos TL. Filtered dynamic matrix control applied to a solar collector field. In: 2015 6th International Renewable Energy Congress (IREC). Sousse, Tunisia: IEEE; 2015. p. 1–6.

Lima, D. M.; Normey-Rico, J. E.; Santos, T. L. M. Temperature control in a solar collector field using Filtered Dynamic Matrix Control. ISA Transactions, v. 62, p. 39–49, 2016. ISSN 00190578. Disponível em: <http://dx.doi.org/10.1016/j.isatra.2015.09.016>.

Normey-Rico, J. E.; Camacho, E. F. Control of Dead-time Processes. 2. ed. [S.l.]: Springer Science & Business Media, 2007.

Roca L, Berenguel M, Yebra L, Alarcón DC. Preliminary modeling and control studies in AQUASOL project. Desalination 2008;222(1–3):466–73.

Roca L, Berenguel M, Yebra L, Alarcón-Padilla DC. Solar field control for desalination plants. Solar Energy 2008;82(9):772–86.

Zheng, J. et al. Solar tracking error analysis of fresnel reflector. Scientific World Journal, Hindawi Publishing Corporation, v. 2014, n. December, 2014. ISSN 1537744X.

Duffie, J. A., Beckman, W. A., 1991. Solar engineering of thermal processes, second ed., John Wiley & Sons, New York

Sánchez A.J., Gallego A.J., Escaño J.M., Camacho E.F., 2018. Event-based MPC for defocusing and power production of a parabolic trough plant under power limitation. Solar Energy, vol. 174, 570-581.

Steinmann, W.-D., Eck, M., 2000. Direct solar steam generation in parabolic troughs: thermal stress due to variations in irradiation. In: Proceedings of the 10th SolarPACES Symposium.